Inorg. Chem. **2005**, *44*, 9817–9822

Structure-Controlled Solventless Thermolytic Synthesis of Uniform Silver Nanodisks

Yu-Biao Chen,[†,‡] Ling Chen,[†] and Li-Ming Wu*[,†]

State Key Laboratory of Structural Chemistry, Fujian Institute of Research on the Structure of Matter, Chinese Academy of Sciences, Fuzhou, Fujian 350002, P. R. China, and Graduate School of the Chinese Academy of Sciences, Beijing 100039, P. R. China

Received July 26, 2005

Monodisperse silver nanodisks are synthesized on the gram scale from a well-characterized layered silver thiolate precursor via thermolysis at 180–225 °C under a N_2 atmosphere. XRD, TEM, HRTEM, and AFM analyses indicate that the nanodisks generated at 180 °C over 2 h have an average diameter of about 16.1 nm ($\sigma = \pm 12\%$) and a thickness of 2.3 nm ($\sigma = \pm 14\%$), and they lie on their (111) faces. The disk shape is considered to be predestined by the crystal structure of the precursor. Important aspects regarding the stability of the precursor, the thermolysis temperature, and the annealing time, as well as a possible conversion mechanism, are discussed.

Introduction

Research in the most interesting field of nanomaterials has been active since late in the last century motivated by the unique properties associated with the nanoscale applications as optical, catalytic, and electronic devices and the fundamental curiosity of scientists.[1] The physical properties of nanomaterials are usually closely related to their shape and size, for example, shape-related anisotropic optical properties, luminescence, conductivity and catalytic activity.[2] Hence, the syntheses of special morphologies have become the primary challenge, and diverse methods have been explored to gain control over particle size and shape.[3] However, attempts to control particle shape have met with only limited success.[4]

The newly established solventless thermolytic method has proven to be successful in producing various nanomaterials, such as Cu_2S,[5] NiS,[6] and Bi_2S_3[7] rods, trigonal prisms, wires, and fabrics. Our previous report[8] demonstrated that the morphology of the nanoproducts could be significantly controlled via the structural state of the precursor used in this method. For example, the viscosity of the colloidal thiolate precursor proved to be a key parameter in controlling the shape of the nanoproducts. Uniform nanowires, nanorods, or nanospheres could be made from the corresponding precursors that came from solutions with different viscosities and thus characteristics of the precursor polymerization. In this paper, we present further developments in this mild conversion to nanoparticles at relatively low temperatures. Under such conditions, the primary distribution of product nuclei and the interparticle aggregations are thought to be influenced largely by the structure of the precursor. Therefore, a structurally anisotropic precursor is very likely to restrict both the initial nuclei concentration and the consequent atom diffusion path and speed and to lead to the formation of an anisotropic nanoproduct. That is, the control

* To whom correspondence should be addressed. E-mail: Liming_Wu@fjirsm.ac.cn. Phone: (011)86-591-83705401. Fax: (011)86-591-83704947.

† Fujian Institute of Research on the Structure of Matter.

‡ Graduate School of the Chinese Academy of Sciences.

(1) (a) Duan, X.; Niu, C.; Sahi, V.; Chen, J.; Parce, J. W.; Empedocles, S.; Goldman, J. L. *Nature* **2003**, *425*, 274−278. (b) Bruchez, M.; Moronne, M.; Gin, P.; Weiss, S.; Alivisatos, A. P. *Science* **1998**, *281*, 2013−2016. (c) Sun, S.; Murray, C. B.; Weller, D.; Folks, L.; Moser, A. *Science* **2000**, *287*, 1989−1992. (d) Wang, J. F.; Gudiksen, M. S.; Duan, X. F.; Cui, Y.; Lieber, C. M. *Science* **2001**, *293*, 1455−1457.

(2) (a) Jin, R.; Cao, Y. C.; Hao, E.; Métraux, G. S.; Schatz, G. C.; Mirkin, C. A. *Nature* **2003**, *425*, 487−490. (b) Murphy, C. J.; Jana, N. R. *Adv. Mater.* **2002**, *14*, 80−82.

(3) (a) Morales, A. M.; Lieber, C. M. *Science* **1998**, *279*, 208−211. (b) Trentler, T. J.; Hichman, K. M.; Geol, S. C.; Viano, A. M.; Gibbons, P. C.; Buhro, W. E. *Science* **1995**, *270*, 1791−1794. (c) Cheon, J.; Kang, N. J.; Lee, S. M.; Lee, J. H.; Yoon, J. H.; Oh, S. J. *J. Am. Chem. Soc.* **2004**, *126*, 1950−1951.

(4) (a) Xia, Y.; Yang, P.; Sun, Y.; Wu, Y.; Mayers, B.; Gates, B.; Yin, Y.; Kim, F.; Yan, H. *Adv. Mater.* **2003**, *15*, 353−389. (b) Jin, R.; Cao, Y.; Mirkin, A. C.; Kelly, K. L.; Schatz, G.; Zheng, J. G. *Science* **2001**, *294*, 1901−1903.

(5) (a) Larsen, T. H.; Sigman, M.; Ghezelbash, A.; Doty, R. C.; Korgel, B. A. *J. Am. Chem. Soc.* **2003**, *125*, 5638−5639. (b) Sigman, M. B.; Ghezelbash, A.; Hanrath, T.; Saunders, A. E.; Lee, F.; Korgel, B. A. *J. Am. Chem. Soc.* **2003**, *125*, 16050−16057.

(6) Ghezelbash, A.; Sigman, M. B.; Korgel, B. A. *Nano Lett.* **2004**, *4*, 537−542.

(7) Sigman, M. B.; Korgel, B. A. *Chem. Mater.* **2005**, *17*, 1655−1660.

(8) Chen, L.; Chen, Y.-B.; Wu, L.-M. *J. Am. Chem. Soc.* **2004**, *126*, 16334−16335.

10.1021/ic051246d CCC: $30.25
Published on Web 11/24/2005

over the shape of the product is achievable through control of the structural character of the precursor. Thus, we have successfully synthesized remarkably uniform silver nanodisks (~16 × 2.3 nm) by this conversion of a layered silver thiolate with a large interlayer spacing of 34.6 Å.

Silver nanoparticles are of particular interest because of the unusual properties and applications presumably associated with their shape and size.[9] A number of methods exhibit excellent control over shape and lead to silver nanocubes, nanowires, nanospheres, nanoprisms, and nanorods.[3a,10] In contrast, layered nanoparticles are less well-known even though such a structural motif is highly desired for advanced applications in light-emitting diodes and biological diagnostics, for example.[9] To date, flat silver nanodisks have come from template,[11] soft colloidal,[12a] solution-phase,[12b] and photoreduction methods.[12c] However, these products show different degrees of coexistence with other shapes, such as triangles and prisms.[12]

Experimental Section

Chemicals. Dodecanethiol ($C_{12}H_{25}SH$) (Labcaster, 98%), triethylamine ($(C_2H_5)_3N$) (A.R. > 99.5%), silver nitrate grains ($AgNO_3$) (Shanghai, A.R. >99.8%), acetonitrile (CH_3CN), (A.R.), ethanol (A.R.), and chloroform (A.R.) were used as purchased without further purification. N_2 gas (99.99%) was purchased from Fuzhou Xinhang Gas Co.

Synthesis of Ag Thiolate Precursor. Silver nitrate ($AgNO_3$, 1.36 g, 8 mmol) was dissolved in 70 mL acetonitrile, and 1.92 mL (16 mmol) of dodecanethiol was added with vigorous stirring, resulting in a white powder precipitate. After the dropwise addition of 1.16 mL (16 mmol) triethylamine to the mixture and another 30 min of stirring, the precipitate was collected by filtration, washed two to three times with acetonitrile to ensure the removal of all soluble materials, and then pumped in a vacuum desiccator to remove residual solvent. The light yellow powder precursor was determined to be a pure layered silver thiolate (see details below), and the yield is about 100% based on $AgNO_3$, indicating that the Ag^+ ions are completely precipitated. Elemental analysis on the dry powder (assumed formula $AgSC_{12}H_{25}$) found (calcd): C, 46.69 (46.74); H, 8.12 (8.18); N, < 0.3 (0); S, 10.40 (10.38). This is reinforced by its presumed stoichiometric synthesis from a 1:1:1 mole ratio of $AgNO_3$/thiol/triethylamine as above which resulted in a structurally identical product judged from the X-ray powder diffraction patterns. The weak base triethylamine used in the synthesis serves to bind protons and accelerate the coordination between Ag^+ and thiols.

Synthesis of Ag Nanodisks. In a representative reaction, the light yellow powdered $AgSC_{12}H_{25}$ precursor in a Pyrex boat was transferred into a long Pyrex tube (6 cm × 1m), capped on both ends, purged with N_2 gas for 5 min, heated in a programmed tube furnace at 180 °C for 2 h, and cooled to room temperature radiantly in the furnace. The product was dispersed in a chloroform/ethanol mixture (v/v ratio about 1:10) and centrifuged at 4,000 rpm for 5 min to remove molecular byproducts. The nanodisk yield was ~52% based on number of moles of AgSR converted to elemental Ag. The reaction conditions for the Ag nanodisks are summarized in Table 1, and more XRD patterns are shown in Supporting Information. Detailed XRD and TEM studies are described below.

Table 1. Experimental Conditions for Preparation of Silver Nanodisks of Different Sizes from $AgSC_{12}H_{25}$

annealing temp (°C)[a]	annealing time (h)	description of products and phase analysis[b]
165	4	black, mainly precursor
180	0.75	black, mainly precursor
180	2	black, fcc Ag nanodisk (16.1 nm ($\sigma = \pm 12\%$))
200	2	black, fcc Ag nanodisk (24.5 nm ($\sigma = \pm 10\%$))
225	2	black, fcc Ag nanodisk (40.6 nm ($\sigma = \pm 15\%$)) + monoclinic Ag_2S (5 nm)

[a] Heating from room temperature to the desired temperature was finished within 2 h. [b] Phase analysis judged from the XRD pattern and the average diameter.

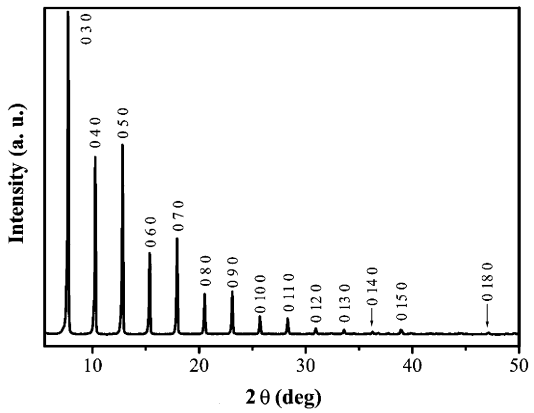

Figure 1. Polycrystalline diffraction pattern (Cu Kα radiation) of the as-synthesized Ag thiolate precursor with the indexes of reflections.

Sample Characterization. Powder X-ray diffraction (XRD), transmission electron microscopy (TEM), high-resolution TEM (HRTEM), and atomic force microscopy (AFM) were used to characterize the structure, composition, size, and shape of the synthesized materials. TEM and HRTEM images were collected using JEOL 2010 TEM equipped with a field emission gun operating at a 200 kV. Images were acquired digitally using a Gatan multipole scanning CCD camera with an imaging software system. All TEM samples were prepared by depositing a drop of dilute nanodisks dispersion in chloroform onto 200 mesh carbon-film-coated Cu grids. Chemical elemental analysis performed by Vario EL III (Elementar Co.). XRD was obtained using a Rigaku DMAX 2500 powder diffractometer with ultra 18 KW Cu radiation. UV−vis spectroscopy was measured on a PerkinElmer Lambda-900 spectrophotometer.

Results and Discussion

Structural Description of $AgSC_{12}H_{25}$ Precursor. The X-ray powder diffraction pattern of the as-synthesized $AgSC_{12}H_{25}$ precursor in Figure 1 shows intense narrow reflections corresponding to successive orders of diffraction

(9) (a) Sun, Y.; Xia, Y. *Science* **2002**, *298*, 2176−2179. (b) Dumestre, F.; Chaudret, B.; Amiens, C.; Renaud, P.; Fejes, P. *Science* **2004**, *303*, 821−823.
(10) (a) Yu, D.; Yam, V. W. *J. Am. Chem. Soc.* **2004**, *126*, 13200−13201. (b) Sun, Y.; Mayers, B.; Herricks, T.; Xia, Y. *Nano Lett.* **2003**, *3*, 955−960. (c) Sun, Y.; Xia, Y. *Adv. Mater.* **2003**, *15*, 695−699. (d) Jana, N. R.; Gearheart, L.; Murphy, C. J. *Chem. Commun.* **2001**, 617−618.
(11) Hao, E.; Kelly, K. L.; Hupp, J. T.; Schatz, G. C. *J. Am. Chem. Soc.* **2002**, *124*, 15182−15183.
(12) (a) Maillard, M.; Giorgio, S.; Pileni, M.-P. *Adv. Mater.* **2002**, *14*, 1084−1086. (b) Maillard, M.; Huang, P.; Brus, L. *Nano Lett.* **2003**, *3*, 1611−1615. (c) Chen, S.; Fan, Z.; Carroll, D. L. *J. Phys. Chem. B* **2002**, *106*, 10777−10781.

from a layered structure with large *d* spacing and preferred orientation. This precursor is structurally analogous to the shorter silver alkylthiolates,[13] AgSR (R = $(CH_2)_nCH_3$, n = 2, 3, 5, 7), which have $\{AgSR\}_\infty$ layers with substituents extending normal to both sides of a central slab of Ag and S atoms. Each central slab is a quasi-hexagonal network constructed of $[Ag_3(SR)_3]$ six-rings. Such geometry gives in-plane Ag−Ag distances of around 4.5 Å. The interlayer distance is found to be in proportion to the length (L_{n+1}) of the substituent, wherein the central Ag/S slab contributes a constant ~1.5 Å. To be consistent with ref 13, we define *b* as the axial direction normal to the layers. The progressions of interlayer reflections (0*k*0) of our $AgSC_{12}H_{25}$ precursor are presented in SI Table 1. There is excellent agreement between the calculated axial lengths (*kd*) for reflections with $3 \le k \le 18$ with an average of 34.6 Å. The proposed formula for the thickness of the complete layers is to be ($2L_{n+1}$ + 1.5 Å), and the lengths of some alkylthiol chains (L_{n+1}) from crystal structure data on $AgS(CH_2)_nCH_3$, are 5.7, 6.9, 9.5, and 11.9 Å for n = 2, 3, 5, and 7, respectively,[13] increasing roughly 1.2 Å per CH_2 group. In our case, ($2L_{n+1}$ + 1.5 Å) for dodecanethiolate would be 34.9 Å, consistent with the observed value (SI Table 1). The small discrepancy may come from a nonzero tilt angle of the long chain with respect to the central slab and no interpenetration at the interface between layers. Such monolayer structural motifs have been observed for thiols on clean gold surfaces but differ significantly in that the Ag−SR bond contrasts with the Au−HSR absorption.[14] A common observation with layered AgSR compounds is that the {0*k*0} reflections get more pronounced with the increase of alkyl chain length, together with the fact that the layered compounds have a high orientation preference (SI Figure 1). The {*h*0*l*} reflections of polycrystalline $AgSC_{12}H_{25}$ are too weak to allow investigation of the intralayer structural details. However, similar bonding patterns and geometry for the Ag/S central slab relative to those of bulk layered silver-thiolates are reasonable.

Ag Nanodisks Converted from a Layered Precursor. Uniform Ag nanodisks are obtained by heating light yellow $AgSC_{12}H_{25}$ powder at 180 °C for 2 h under N_2 flow; the product turned black during the firing. The Ag^+ is thought to be reduced by the thiolate (SR^-) through the electron transfer from the thiolate (SR^-) to silver cation; then two SR radicals yield the disulfide shown in the following equations.[15]

$$AgSR \xrightarrow{\Delta} Ag + SR^{\bullet}$$

$$2SR^{\bullet} \rightarrow RSSR$$

After it was washed with a chloroform/ethanol mixture, the black powder was identified as single-phase face-centered-cubic silver (ICSD #64706) by XRD (Figure 2), and its TEM images (Figure 3) show a remarkably monodisperse nanodisk morphology. To gain insight into the mechanistic basis behind this unusually efficient conversion, we investigated the importance of two reaction conditions: reaction temperature and time. Several reactions carried out at 140 °C for 8 h, 165 °C for 2 h, and 180 °C for 0.75 h produce dark yellow powders. Their XRD patterns (SI Figure 1) contain all the axial reflections of the layered precursor and no other detectable phases, although the color change does imply the formation of small amounts of silver. However, the absence of XRD signals and the invisibility of crystals by TEM observation indicate that the silver in these three reactions is still poorly crystalline or amorphous. An optimum synthesis condition is heating the precursor for 2 h at 180 °C, but uniform Ag nanodisks are repeatedly produced by firing for 2 h in the temperature range between 180 °C and 225 °C (Table 1). As expected, the diameters of the nanodisks increase (from 16.1 to 40.6 nm) (SI Figures 2−5) with the temperature increase, but the morphology remains strikingly uniform. An efficient mechanism for this one-to-one (layered precursor to nanodisk) conversion will be discussed below. We also found that at ≥225 °C, a second major phase, Ag_2S (acanthite, ICSD#30445), is formed. Above 250 °C, no silver is formed.

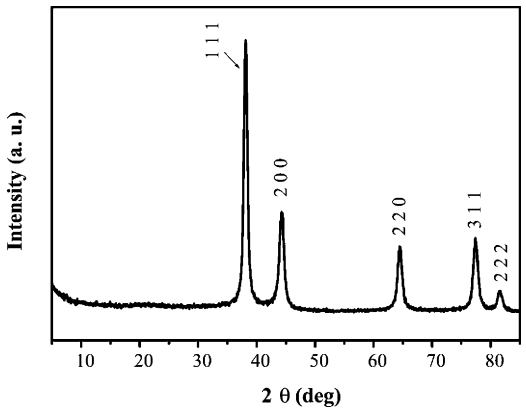

Figure 2. XRD pattern of Ag nanodisks produced at 180 °C for 2 h. All peaks are indexed as face-centered-cubic silver.

Characterization. TEM images for the as-synthesized nanodisks prepared at 180 °C for 2 h (Figure 3) reveal a strikingly uniform morphology with an average diameter of 16.1 nm ($\sigma = \pm$ 12%) nm (SI Figure 3). The disk shapes have been obtained before under different experimental conditions,[11,12] but not with such monodispersity in shape and size. The EDX from a nanodisk shown in Figure 3 on a Cu grid indicates only pure silver (SI Figure 7), and the single-phase purity is confirmed by the XRD result (Figure 2). The HRTEM image of Ag nanodisks in Figure 4b shows Ag atoms with close-packed hexagonal symmetry and an interlayer distance of 2.37 Å, corresponding to the (111) layer spacing of fcc silver. Figure 4c shows a model (111) image of fcc silver. The Fourier transform (FFT) of the image in Figure 4a gives a decent description of the crystal orientation, and the 6-fold {111} and 4-fold {002} reciprocal points are marked in Figure 4d. The measured values of d_{111} and d_{002}(2.37 and 2.04 Å, respectively) are in agreement with

(13) Dance, I. G.; Fisher, K. J.; Banda, R. M. H.; Scudder, M. L. *Inorg. Chem.* **1991**, *30*, 183−187.
(14) Porter, M. D.; Bright, T. B.; Allara, D. L.; Chidesey, C. E. D. *J. Am. Chem. Soc.* **1987**, *109*, 3559−3568.
(15) Oae, S. *Organic Sulfur Chemistry: Structure and Mechanism*; CRC Press: Boca Raton, FL, 1991; Chapter 6, pp 204−206.

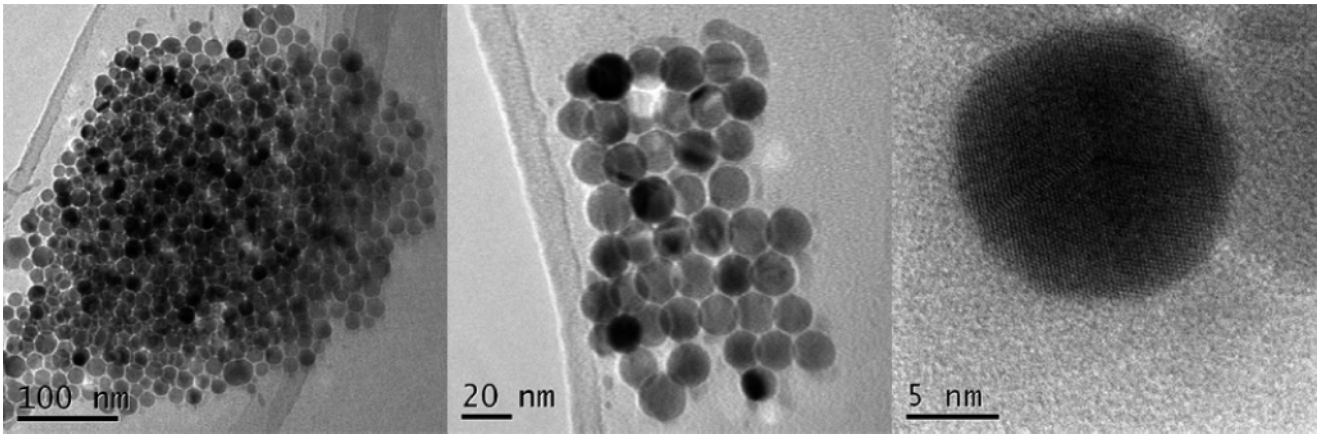

Figure 3. Ag nanodisks converted from the layered $AgSC_{12}H_{25}$ precursor at 180 °C for 2 h.

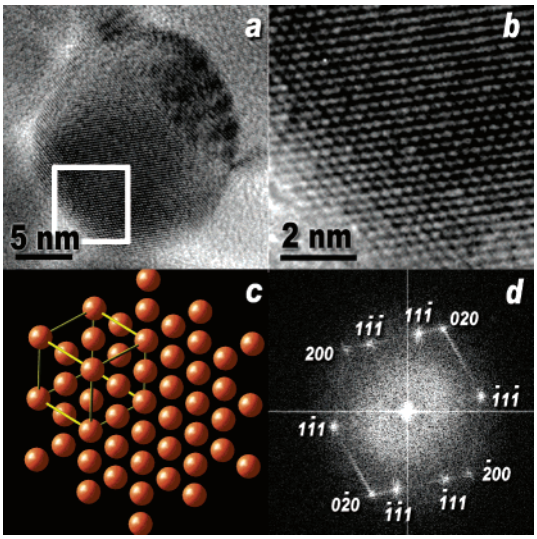

Figure 4. (a) HRTEM image of Ag nanodisks produced at 180 °C for 2 h. (b) An enlarged image of the selected part of panel a. The hexagonally arranged spots correspond to the close-packed (111) layers of face-centered-cubic silver. (c) A [111] projection of the cubic silver structure with the unit cell marked, and a (d) FFT of the imaged nanodisk in panel a demonstrating crystal orientation.

bulk crystallographic data ($a = 4.08$ Å, ICSD #64706). The lattice parameter is calculated to be 4.12 Å from this pattern, which is similar to the value of 4.17 Å in ref 12a and that of 4.08 Å for bulk silver. All nanodisks appear as layered and lying on their (111) faces. The average diameter by TEM is 16.1 nm (Figure 3). The TEM images indicate that all of the nanoparticles are nummular, which suggests only two possibilities: they are either perfect spheres or have large diameter/height (D/H) ratios, disklike morphologies, and lie on their faces. AFM is further used to define the morphology of nanoparticles (Figure 5). The line analysis at the bottom indicates that this disk has a thickness 2.2 nm and diameter of 18 nm, consistent with the TEM observations. The thickness and diameter value for the individual disks give a large D/H ratio of about 7, $\text{diameter}_{(av)} = 16.1$ nm ($\sigma = \pm$ 12%) and $\text{height}_{(av)} = 2.3$ nm ($\sigma = \pm$ 14%) (SI Figures 3 and 6); therefore, we define the as-made Ag particles as nanodisks. Of course, with such large D/H ratios, it is difficult for the nanodisks to stand on their edges. It is important to notice the curved top surfaces of these nanodisks, which are

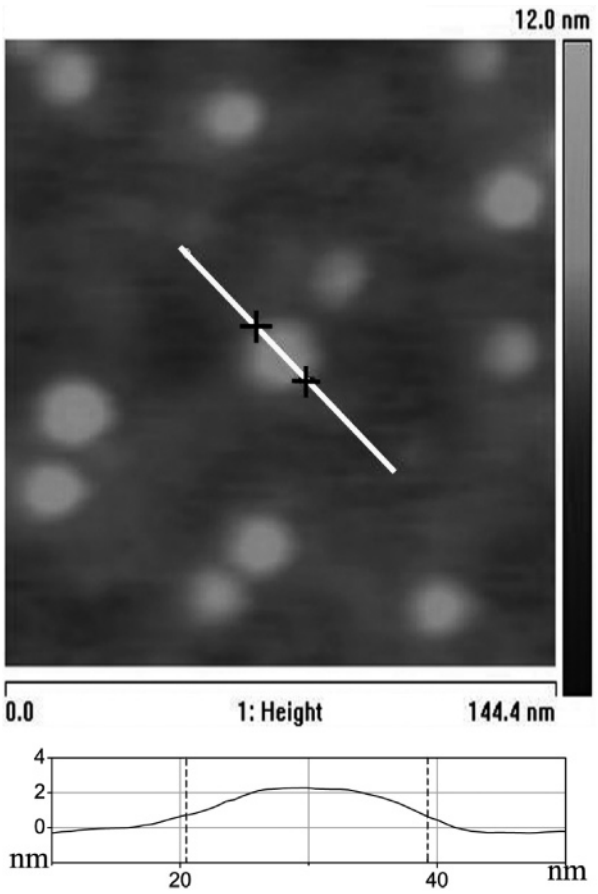

Figure 5. (top) AFM images of the Ag nanodisks produced at 180 °C for 2 h, and (bottom) the height profile along the line in the top figure. The height is about 2.2 nm.

significantly different than the flatness of the Ag nanoprisms[4b] and other nanodisks.[12a] The aspect ratio of the last are 4−5.5 for the truncated hexagonal or pseudo-hexagonal Ag disk.[12a] The average diameter of the as-made Ag nanodisks increases to 24.5 nm at 200 °C and to 40.6 nm at 225 °C for 2 h (SI Figures 4 and 5). The nanodisks show an absorption band at ca. 413 nm (Figure 6), typical of the plasmon resonance of the spherical silver nanoparticles, since the nanodisks assumed a rounded rather than sharply angular surfaces as do triangles or prisms.[4b,12] This is similar to the phenomenon found with silver nanocubes.[10a]

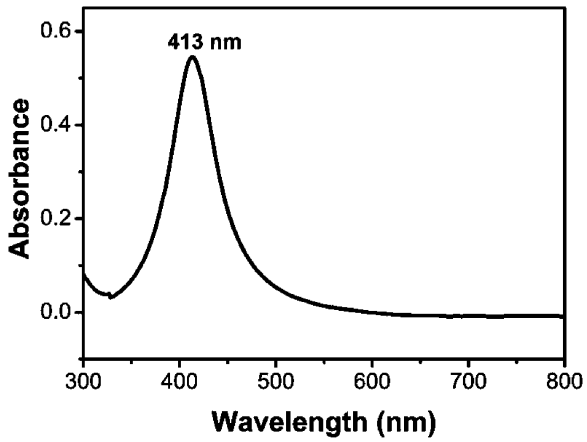

Figure 6. Room-temperature UV−vis absorption spectrum of the chloroform suspension of Ag nanodisks produced at 180 °C for 2 h.

Possible Conversion Mechanism. The Ag nanodisks are successfully formed from the thiolate precursor by thermolysis between 180 and 225 °C for an appropriate period of time. A lower temperature or a shorter time regularly produces a dark-yellow powder that possesses an identical XRD pattern to that of the precursor (SI Figure 1). $AgSC_{12}H_{25}$ has been reported to exhibit a columnar rather than a lamellar structure from 130 to 180 °C in air without any decomposition, and the different heating rates or preparation procedures were found to have noticeable influences on the temperatures at which the different mesophases of $AgSC_{12}H_{25}$ appeared.[16] To examine the $AgSC_{12}H_{25}$ structure under our heating conditions, another reaction was carried out in which crystalline $AgSC_{12}H_{25}$ was heated in air at 155 °C for 2 h, and then immediately quenched in liquid N_2 to freeze the precursor structure. The XRD pattern taken right after quenching (SI Figure 8a) showed a layered structure with an interlayer spacing of 34.6 Å consisted with the room-temperature structure (Figure 1) and the results in SI Figure 1. Thereafter, the dark-red synthesized product was dispersed and washed in a chloroform/ethanol mixture to get rid of most of the organic components. The XRD pattern of the precipitate (SI Figure 8b) make it clear that Ag has formed under such conditions which indicates that decompostion of $AgSC_{12}H_{25}$ occurred. In other words, the experimental conditions in ref 16 led to different results from ours in that they only found a crystal-to-micellar transformation. This suggests that the experimental conditions are crucial to the chemical behavior of the Ag thiolate, especially, under thermolysis condition. On the basis of these facts, it is reasonable to regard the structure of the $AgSC_{12}H_{25}$ precursor under our firing conditions to still be a layered structure while its decomposition occures.

We thus hypothesize that the conversion mechanism contains two processes: nucleation and growth. On the first heating, the AgSR partly decomposes to small metallic silver clusters that serve as nuclei for the further reaction stages, and their distribution inherits the layered pattern of the mother structure. Second, the subsequent nanoparticle growth is fulfilled by atom diffusion which is guided by the concentration gradient of the Ag atoms. The Ag atom distribution, constrained by the structure motif of the precursor, has a layered pattern, and the in-plane Ag atoms diffuse isotropically; naturally, the intraplane silver atom aggregation is identical in two directions. In contrast, the interplane silver atom diffusion is hindered by the organic chains, and this diffusion path (34.6 Å initially, Figure 1) is much longer than the intraplane one. Thus, the interplane aggregation is much slower, leading to the formation of a disklike morphology. This mechanism explains the monodisperse morphology of the nanodisk product (Figure 3) well because the Ag atom concentration is self-controlled by the structure of the AgSR precursor, and it is evenly distributed on a atomic level under the mild reaction conditions.

Structure-Controlled Solventless Method. We present here some experimental facts to illustrate our structure-controlled solventless method for converting a layered precursor to the layered nanoproduct. The key character of this approach is that it is a mild conversion, and the reactions can be regarded as a quasi-solid-state process. As is usual in solid-state reactions,[17] the nucleation of the desired product may be relatively easy, and the subsequent growth or thickening of the product is more difficult and mainly determined by atomic diffusion. The molecular structure of the precursor influences the diffusion speed and path of atoms as described above. A structure determination for the solid-state precursor in this method is practical, baring any intervening processes, and we are able to chose/design a precursor structurally to rationally achieve the desired morphology of the nanoproduct. Furthermore, other motifs would be expected if other pronouncedly anisotropic morphologies could be formed for the precursor giving nanobelts, nanorings, etc. Control of the structure of the precursor on the basis of traditional coordination chemistry is more governable and advantageous, and the diversity of known coordination structure types is prominent.[18] Our discoveries of a dependence of the nanoproduct morphology on the precursor structure should also be effective in the preparation of nanoparticles of main group elements with special shapes, such as Bi nanocubes, nanofibers, and nanodisks. And this novel method is also expected to give nanoparticles with heterometal mixing on an atomic scale.

Conclusions. Monodisperse Ag nanodisks with an aspect ratio of 7 have been successfully synthesized giving convincing experimental support for our new structure-controlled solventless method. Silver clusters formed during the *in situ* reduction of layered silver thiolate are nuclei for the nanodisk formation, which involves anisotropic growth perpendicular to (111) face of fcc silver. One of the key points of this process is that the nanoproduct morphology is self-controlled on the atomic level by the structure of the precursor during the mild conversion. This method for the synthesis of layered silver nanodisks is simple, inexpensive, and suitable for production on a gram scale. It is also applicable to the

(16) Baena, M. J.; Espinet, P.; Lequerica, M. C.; Levelut, A. M. *J. Am. Chem. Soc.* **1992**, *114*, 4182−4185.
(17) West, A. R. *Basic Solid State Chemistry*; Wiley: New York, 1999; Chapter 9, pp 408−411.
(18) Henkel, G.; Krebs, B. *Chem. Rev.* **2004**, *104*, 801−824.

synthesis of other layered metallic nanoparticles such as Bi or Au and for salts such as Bi_2S_3, Cu_2S, etc.[19] In addition, the method opens up new possibilities and considerations for the shape control of nanoparticles. More experiments are ongoing to extend the application of this method and to deepen our understanding of the method.

Acknowledgment. We thank Professor John D. Corbett for proof reading. This research was supported by the National Natural Science Foundation of China under Projects 20401014 and 20401013 and the State Key Laboratory Science Foundation under Projects 050086 and 050097. We also thank F. Bao and C.-P. Yang for the assistance with the TEM and AFM measurements.

Supporting Information Available: Additional XRD patterns, size distributions, and EDX results. This material is available free of charge via the Internet at http://pubs.acs.org.

(19) Chen, J.; Chen, L.; Wu, L.-M. Unpublished results.

IC051246D